Journal of Neurochemistry

JOURNAL OF NEUROCHEMISTRY | 2010 | 115 | 748–758 doi: 10.1111/j.1471-4159.2010.06964.x

Cerebellar lipid differences between R6/1 transgenic mice and humans with Huntington's disease

Christine A. Denny,*[1,2] Paula A. Desplats,†,[1,3] Elizabeth A. Thomas† and Thomas N. Seyfried*

*Department of Biology, Boston College, Chestnut Hill, Massachusetts, USA

†Department of Molecular Biology, The Scripps Research Institute, La Jolla, California, USA

Abstract

Huntington's disease (HD) is a progressive neurodegenerative disorder characterized by motor, psychiatric, and cognitive abnormalities. In this present study, we tested whether abnormal motor behavior in a mouse model of HD, the R6/1 transgenic (Tg) mice, was associated with changes in cerebellar lipid composition and gene expression. We report altered motor behavior, which was associated with abnormal expression of glycosyltransferase genes in the cerebellum of R6/1 Tg mice. Cerebellar wet weight and total ganglioside concentration was significantly lower in R6/1 Tg mice than in wild-type (Wt) mice. Furthermore, the Purkinje cell-enriched ganglioside LD1 and the granule cell-enriched ganglioside GD1a were significantly lower in R6/1 Tg mice than in Wt mice. The myelin-enriched lipid sulfatides was also reduced in the cerebellum of R6/1 Tg mice. In contrast to the R6/1 Tg mice, total cerebellar ganglioside concentration did not differ between HD and control subjects. However, expression of several cerebellar glycosyltransferases genes was significantly less in HD subjects than in control subjects. Our findings indicate that the R6/1 Tg mice have severe cerebellar glycosphingolipid (GSL) abnormalities that may account, in part, for their abnormal motor behavior. Although the cerebellar lipid abnormalities found in the R6/1 Tg mice were not found in these HD subjects, the R6/1 Tg mice may be useful for evaluating the role of GSLs in cerebellar development.

Keywords: ganglioside, cerebellum, cerebrosides, qPCR, Purkinje cell, sulfatides.

J. Neurochem. (2010) **115**, 748–758.

Gangliosides are a family of sialic acid-containing glycolipids that are present in most vertebrate cells and tissues (Ledeen 1983). Previous studies have shown that ganglioside differences exist between neuronal cells and glial cells (Byrne *et al.* 1988); between different types of glial cells (Raff *et al.* 1983; LeVine and Goldman 1988); and between resting and reactive glia (Seyfried and Yu 1985). Previous studies in cerebellar mouse mutants have shown that ganglioside GD1a is enriched in mature granule cells (Seyfried and Yu 1984; Furuya *et al.* 1994); that disialosyl paragloboside LD1/GT1a is enriched in Purkinje cells (Seyfried and Yu 1984; Chou *et al.* 1990); and that ganglioside GT1b is concentrated in both cell types (Seyfried *et al.* 1983; Seyfried and Yu 1990). In addition to gangliosides, other lipids, such as cerebrosides and sulfatides, are reliable markers of myelin content and composition (Seyfried and Yu 1980; Muse *et al.* 2001; Denny *et al.* 2006). Hence, glycosphingolipids (GSLs) can be indicators for assessing the neural integrity of the mouse cerebellum.

Huntington's disease (HD) is an autosomal dominant, progressive neurodegenerative disorder characterized by motor, psychiatric, and cognitive abnormalities (The Huntington's Disease Collaborative Research Group 1993; Bates 2001; Bolivar *et al.* 2004). The onset of symptoms is generally in midlife, with death occurring 10–20 years thereafter (Harper 1996). HD is caused by an abnormal expansion of a cytosine, adenine, guanine (CAG) trinucleotide repeat in exon 1 of the HD gene, located on the short arm of chromosome 4 (Gusella *et al.* 1983; The Huntington's Disease Collaborative Research Group 1993). Although normal individuals have less than 35 CAG repeats, HD patients have 36 or more CAG repeats. This CAG

Received May 17, 2010; revised manuscript received August 17, 2010; accepted August 17, 2010.

Address correspondence and reprint requests to Thomas N. Seyfried, PhD, Boston College, Biology Department, Chestnut Hill, MA 02467, USA. E-mail: thomas.seyfried@bc.edu

[1]These authors contributed equally to this work.

[2]Current affiliation: Department of Biological Sciences, Columbia University, New York, New York, USA

[3]Current affiliation: Department of Neurosciences, University of California, San Diego, La Jolla, California, USA

expansion results in an abnormally long stretch of polyglutamine residues in the encoded protein huntingtin (htt). Although htt is widely expressed in both brain and peripheral tissues (e.g. the testes), its specific function is still poorly understood (Trottier *et al.* 1995; DiFiglia *et al.* 1997; MacDonald 2003; MacDonald *et al.* 2003; Imarisio *et al.* 2008).

The typical neuropathological hallmarks of HD include neuronal loss and gliosis in the caudate nucleus and putamen (Vonsattel and DiFiglia 1998). Abnormalities have also been reported in the cerebellum of HD patients, especially in those afflicted at juvenile ages (Jervis 1963; Byers *et al.* 1973; Rodda 1981; Hattori *et al.* 1984; Hayden and Kremer 1995; Ruocco *et al.* 2006; Paradiso *et al.* 2008). There is considerable variability in the pathology observed in those patients with cerebellar involvement. Incoordination, ataxia, tremors (Markham 1969), and Purkinje cell loss (Jeste *et al.* 1984) have also been associated with cerebellar malfunction in some HD patients. Moreover, recent imaging analysis showed cerebellar atrophy of gray and white matter, with white matter loss being greater than gray matter loss (Fennema-Notestine *et al.* 2004). In contrast to the considerable information on the neuropathology and neurochemistry of the caudate nucleus and the putamen in HD, less is known about the neurochemistry of the cerebellum in HD.

The R6/1 mouse is a murine model for HD and expresses exon 1 of the human HD gene containing an expanded number of CAG repeats (Mangiarini *et al.* 1996). These mice exhibit abnormal rotarod performance, hind limb clasping, and hypoactivity suggestive of cerebellar abnormalities (Mangiarini *et al.* 1996; Naver *et al.* 2003). The behavioral abnormalities in these mice usually appear by 15–21 weeks of age, with death occurring by 32–40 weeks of age. Similar to HD patients, the R6/1 transgenic (Tg) mice exhibit involuntary jerky shudders that resemble chorea and display weight reductions at approximately 22 weeks of age, following motor impairments (Mangiarini *et al.* 1996; Naver *et al.* 2003). No previous studies have evaluated cerebellar neurochemistry in the R6/1 Tg mice.

In this study, we investigated for the first time the total cerebellar lipid composition of R6/1 Tg mice and of HD subjects, to include gangliosides, neutral lipids, and acidic lipids. The objective of this study was to determine whether previous observations of abnormal motor behavior in R6/1 Tg mice might be associated with changes in cerebellar lipid composition. Our results show marked cerebellar GSL abnormalities and abnormal expression of glycosyltransferases genes in R6/1 Tg mice. Although the content and composition of lipids was generally similar in the cerebellum of wild-type (Wt) mice and control human subjects, the lipid changes seen in the cerebellum of R6/1 Tg mice were not seen in the cerebellum of these human HD subjects. Further studies will be necessary to assess cerebellar GSLs in human HD subjects.

Materials and methods

Mice

Huntington's disease (HD) R6/1 transgenic (Tg) mice generated by Professor Gillian Bates (Mangiarini *et al.* 1996), which express exon 1 of the human HD gene carrying 116 CAG repeats, were obtained from The Jackson Laboratory (Bar Harbor, ME, USA) ('B6CBACaTg(HDexon1)61Gpb/J'). Mouse genotyping was performed at 4 weeks of age to verify CAG repeat length according to the Jackson Laboratory protocol. The mice were reared in a colony at The Scripps Research Institute (La Jolla, CA, USA). The room temperature was maintained at 22°C on a 12 h light/12 h dark cycle on at 07:00 hours. Food and water were provided throughout the experiment *ad libitum*. All animal experiments were carried out with ethical committee approval in accordance with the National Institutes of Health Guide for the care and use of laboratory animals and were approved by the Institutional Animal Care and Use Committees of The Scripps Research Institute.

Human subjects

Human post-mortem cerebellum samples were obtained from the Harvard Brain Tissue Resource Center (McLean Hospital, Belmont, MA, USA; http://www.brainbank.mclean.org/). Cerebellum samples consisted of three HD samples, grade 3, and three controls. Samples were matched for age and sex. All samples were stored at −80°C until use.

Footprint test

The footprint test was used to compare the gait of wild-type (Wt) mice with R6/1 Tg mice as previously described (Carter *et al.* 1999). Briefly, the hind- and forefeet of Wt and R6/1 Tg mice (6 months of age) (n = 10 mice/group; male and female) were coated with purple and orange non-toxic paints, respectively. A fresh sheet of white paper was placed on the floor of the runway for each run. The footprint patterns were analyzed for four different step parameters. Stride length was measured as the average distance of forward movement between each stride. Hind paw-base width and front paw-base width were measured as the average distance between left and right hind footprints and left and right front footprints, respectively. To determine these values, the perpendicular distance of a given step to a line connecting opposite preceding and proceeding steps was measured. Distance from left or right front footprint/hind footprint overlap was used to measure uniformity of step alternation. When the center of the hind footprint fell on top of the center of the preceding front footprint, a value of zero was recorded. When the footprints did not overlap, the distance between the center of the footprints was recorded. For each step parameter, three values were measured from each run, excluding footprints made at the beginning and end of the run where the animal was initiating and finishing movement, respectively. The mean value of each set of three values was used in subsequent analysis.

Tissue processing

The Wt and R6/1 Tg mice (7–8 months of age) (n = 3 mice/group; female) were killed by cervical dislocation under halothane inhalation. Brains were dissected and frozen immediately. The cerebella were stored at −80°C and were then lyophilized to obtain dry weights.

Lipid isolation, purification, and quantification

Total lipids were isolated and purified from lyophilized cerebellum by using modifications of previously described procedures (Seyfried *et al.* 1978; Hauser *et al.* 2004; Denny *et al.* 2006). Neutral and acidic lipids were separated by using DEAE-Sephadex (A-25; Pharmacia Biotech, Upsala, Sweden) column chromatography as previously described (Macala *et al.* 1983; Seyfried et al. 1984a; Kasperzyk *et al.* 2005; Denny *et al.* 2006). The total lipid extract, suspended in solvent A ($CHCl_3$: CH_3OH : H_2O, 30 : 60 : 8 by vol), was then applied to a DEAE-Sephadex column (1.2 mL bed volume) that had been equilibrated with solvent A. The column was washed twice with 20 mL of solvent A, and the entire neutral lipid fraction, consisting of the initial eluent plus washes, was collected. This fraction contained cholesterol, phosphatidylcholine, phosphatidylethanolamine, plasmalogens, ceramide, sphingomyelin, and cerebrosides. The acidic lipids were then eluted from the column with 30 mL solvent B ($CHCl_3$: CH_3OH : 0.8 M Na acetate, 30 : 60 : 8 by vol). This fraction contained the gangliosides and other less hydrophilic acidic lipids, including free fatty acids, cardiolipin, phosphatidylserine, phosphatidylinositol, phosphatidic acid, and sulfatides. The gangliosides were isolated and purified from other acidic lipids and analyzed by using the resorcinol assay as we previously described (Hauser *et al.* 2004; Kasperzyk *et al.* 2004). The ganglioside fraction contained GM1, GD3, GD1a, LD1 (mouse only), GD2 (human only), GD1b, GT1b, and GQ1b.

High-performance TLC

All lipids were analyzed qualitatively by high-performance thin-layer chromatography (HPTLC) according to previously described methods (Ando *et al.* 1978; Seyfried *et al.* 1978; Macala *et al.* 1983; Kasperzyk *et al.* 2005; Denny *et al.* 2006). Lipids were spotted on 10- × 20-cm Silica gel 60 HPTLC plates (E. Merck, Darmstadt, Germany) using a Camag Linomat V auto-TLC spotter (Camag Scientific Inc., Wilmington, NC, USA). To enhance precision, an internal standard (oleoyl alcohol) was added to the neutral and acidic lipid standards and samples as previously described (Macala *et al.* 1983; Kasperzyk *et al.* 2005). Purified lipid standards were purchased from Matreya Inc. (Pleasant Gap, PA, USA) or Sigma (St Louis, MO, USA) or were a gift from Dr Robert Yu (Medical College of Georgia, Augusta, GA, USA). The HPTLC plates were sprayed with the resorcinol–HCl reagent and heated at 95°C for 30 min to visualize gangliosides (Kasperzyk *et al.* 2005). For neutral or acidic phospholipids, the plates were developed to a height of either 4.5 or 6 cm, respectively, with chloroform : methanol : acetic acid : formic acid : water (35 : 15 : 6 : 2 : 1 by vol), then developed to the top with hexanes : diisopropyl ether : acetic acid (65 : 35 : 2 by vol) as previously described (Macala *et al.* 1983; Seyfried *et al.* 1984a). Neutral and acidic lipids were visualized by charring with 3% cupric acetate in 8% phosphoric acid solution, followed by heating in an oven at 160–170°C for 7 min. The percentage distribution of the individual lipid bands was determined by scanning the plates on a Personal Densitometer SI with ImageQuant software (Molecular Dynamics, Sunnyvale, CA, USA) for gangliosides, acidic lipids, and neutral lipids.

RNA preparations

Total cerebellar RNA was prepared from symptomatic R6/1 Tg mice and from Wt littermate controls (8 months of age) (n = 5 mice/group; male). RNA extraction and purification was done using NucleoSpin RNA Kit (BD Biosciences, San Jose, CA, USA) according to the manufacturer's instructions. Total cerebellar RNA was prepared from human post-mortem subjects (approximately 100 mg) (n = 3 subjects/group). RNA was purified using Versagene RNA Purification System (GENTRA Systems, Minneapolis, MN, USA) according to the manufacturer's instructions. All the samples were treated with DNAseI to eliminate genomic DNA contamination. RNA quantification was determined by spectrophotometer readings. The ratio of OD_{260}/OD_{280} was used to evaluate the purity of the nucleic acid samples, and the quality of the extracted total RNA was determined using agarose gel electrophoresis. RNA yields were comparable across all HD and control samples.

Real-time PCR analysis

For cDNA synthesis, 1 μg of total RNA from mouse or human samples was reverse transcribed using SuperScript III First-Strand Synthesis System (Invitrogen, Carlsbad, CA, USA) per the manufacturer's protocol. Specific primers for each sequence of interest and for mouse and human internal controls were designed using Primer Express® 1.5 software (Applied Biosystems, Foster City, CA, USA), and their specificity to bind the desired sequence was analyzed by BLAST analysis against the NCBI databases. Standard curves were generated for each gene of interest using serial dilutions of mice or human cDNAs. All primers used showed efficiencies between 90% and 118%, and R^2 values > 0.97, parameters calculated by linear regression analysis of the C_t versus log[template] blots using Graph Pad Prism 3.0 software (La Jolla, CA, USA).

Real-time PCR experiments were performed using the ABI PRISMs 7900HT Sequence Detection System (Applied Biosystems). Amplification was performed on a cDNA amount equivalent to 25 ng total RNA with 1× SYBR Green universal PCR Master mix (Applied Biosystems) containing dNTPs, $MgCl_2$, AmpliTaq Gold DNA polymerase, and forward and reverse primers. Experimental samples and no-template controls were all run in duplicate. The PCR cycling parameters were: 50°C for 2 min, 95°C for 10 min, 40 cycles of 94°C for 15 s, and 60°C for 1 min. Finally, a dissociation protocol was performed at the end of each run to verify the presence of a single product with the appropriate melting point temperature for each amplicon. To further ascertain the specificity and size of the PCR products, the products were run alongside molecular weight markers on a 2% agarose gel in 1× TAE. Quantification of transcript levels in each sample was calculated using SDS2.1 software (Applied Biosystems) by the comparative threshold cycle (C_t) method and expressed as $2\exp(-\Delta\Delta C_t)$ using hypoxanthine guanine phosphoribosyl transferase as an internal control for the mouse sequences, whereas β-2-microglobulin was used for the human sequences. Expression of the β-2-microglobulin and hypoxanthine guanine phosphoribosyl transferase gene was reported as unchanged in HD mice in a previous microarray analysis (Desplats *et al.* 2006). For calculations applying C_t method, expression values from Wt littermate controls of R6/1 Tg mice, or expression values from the control human subjects were used as calibrator samples.

Histology

The Wt and R6/1 Tg mice were perfused with 4% paraformaldehyde (PFA) (6–8 months of age) (n = 3 mice/group; male and female). Brains were dissected and frozen immediately. The cerebella were stored at −80°C until being embedded in paraffin, sectioned at 5 μm, and stained with haematoxylin & eosin (H&E) at the Harvard University Rodent Histopathology Core Facility (Boston, MA, USA). Slides were examined using a Zeiss Axioplane 2 Imaging universal microscope (Zeiss, Thornwood, NY, USA) and a Spot Insight 4MP Fireware Color 3-shot digital camera and Spot software (Diagnostic Instruments, Sterling Heights, MI, USA). A minimum of three randomized images were taken for each mouse cerebellum. Purkinje cells were counted along 200 μm increments that ran parallel to the cerebellar cortex, with the average number of 200 μm increments being 15/mouse. The total number of Purkinje cells counted for each mouse was summed for each individual image.

Statistical analysis

A two-tailed t-test was used to evaluate the significance of differences between the Wt and R6/1 Tg mice, and the HD and control subjects. A one-sample t-test (confidence interval 95%) was performed against a hypothetical value of 1 to assess significant differences between expression of each gene in Wt and R6/1 Tg mice. Statistical analyses were performed using Prism software or using StatView 5.0 software (SAS Institute, Cary, NC). In each figure, n designates the number of individual mice or human cerebellum subjects analyzed.

Results

Motor deficits in R6/1 Tg mice

Gait abnormalities were assessed by analyzing the footprint pattern of mice while they walked along a narrow corridor. Footprint patterns of Wt and R6/1 Tg mice (7–8 months of age) are illustrated in Fig. 1a. The Wt mice walked in a straight line with an even alternating gait. As with most Wt mice, the mice placed the hindpaw precisely at the position where the ipsilateral forepaw had been in the previous step. In contrast to Wt mice, R6/1 Tg mice progressively weaved from side to side, had unevenly spaced shorter strides, and displayed staggering movements (Fig. 1a).

The footprint patterns were assessed quantitatively by four measurements: stride length (Fig. 1b), front footprint/hind footprint overlap (Fig. 1c), forepaw base width (Fig. 1d), and hindpaw base width (Fig. 1e). R6/1 Tg mice displayed a significantly shorter stride length and a significantly greater overlap between front footprint/hind footprint when compared with Wt mice ($p < 0.05$). The forepaw and hindpaw base width was similar in the R6/1 Tg and the Wt mice.

Cerebellar histology of R6/1 Tg mice

Purkinje cell morphology and density was evaluated since Purkinje cells are affected in a range of disorders that exhibit symptoms including: ataxia, chorea, or altered gait. Purkinje cells appeared normal in Wt mice, as they were densely stacked within the cerebellar cortex. In contrast, the Purkinje cells of R6/1 Tg mice had irregularly shaped nuclei (Fig. 2a). Furthermore, the number of Purkinje cells was significantly reduced in the R6/1 Tg mice when compared with the Wt mice (Fig. 2b) ($p < 0.05$). These findings indicate a severe Purkinje cell abnormality in the cerebellum of R6/1 Tg mice.

GSL gene expression in R6/1 Tg mice

We next performed quantitative real-time PCR (qPCR) on isolated cerebellar RNA. (*N*-acetylneuraminyl)-galactosyl-

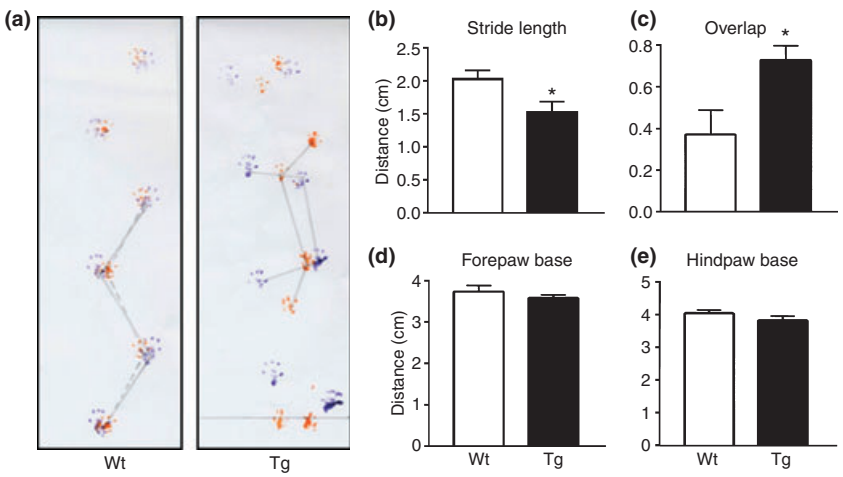

Fig. 1 Footprint analysis of R6/1 mice. Representative walking footprint patterns of Wt and R6/1 Tg mice (a). Qualitatively, the generated patterns clearly differ showing that R6/1 Tg mice displace irregularly space strides and uneven left-right step patterns as compared with the evenly spaced footprints of the Wt mice. Whereas stride length (b) and overlap (c) are significantly altered in R6/1 Tg mice, forepaw (d) and hindpaw (e) base are not significantly altered in the R6/1 Tg mice when compared with Wt mice. *$p < 0.05$. Values represent mean ± SEM (n = 10 mice/group).

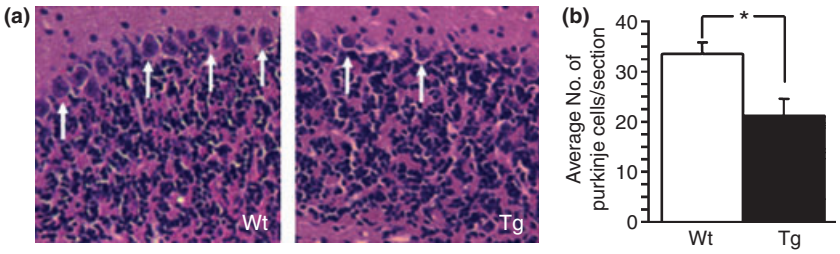

Fig. 2 H&E staining of cerebellar Purkinje cells in Wt and R6/1 Tg mice (a). Images shown at 200×. Arrows indicate cerebellar Purkinje cells. The number of Purkinje cells was significantly reduced in R6/1 Tg mice when compared with Wt mice (b). *$p < 0.05$. Values represent mean ± SEM. ($n = 3$ mice/group).

glucosylceramide *N*-acetylgalactosaminyltransferase (Galgt1; *GalNAcT*; B4GALNT1) and UDP-glucose : ceramide glucosyltransferase (Ugcg) were significantly reduced in R6/1 Tg mice when compared with Wt mice ($p < 0.05$) (Fig. 3a). However, SiaT8a (GD3 synthase; ST8SIA1); SiaT9 (GM3 synthase; ST3GAL5); GLRX2 (glutaredoxin 2), which is part of a family of glutathione-dependent hydrogen donors that participate in a variety of cellular redox reactions; and Ugt8 (UDP glycosyltransferases 8), which catalyzes the transfer of galactose to ceramide, a key enzymatic step in the biosynthesis of galactocerebrosides, were not significantly reduced in R6/1 Tg mice when compared with Wt mice. As Ugcg catalyzes the first glycosylation step in GSL biosynthesis and the product glucosylceramide is the core structure of more than 300 GSLs, we predicted that cerebellar lipids would be significantly altered in R6/1 Tg mice.

Cerebellar lipids of R6/1 Tg mice

We next determined if the motor deficits, Purkinje cell loss, and altered gene expression seen in the R6/1 Tg mice were associated with changes in cerebellar lipid content and distribution. Cerebellar wet weight and total cerebellar ganglioside concentration were significantly lower in R6/1 Tg mice than in Wt mice (Table 1) ($p < 0.05$). The cerebellar water content, a general marker for brain maturation and myelin content (Seyfried 1979; Seyfried and Yu 1980), was slightly higher in the R6/1 Tg mice than in the Wt mice, but the difference did not reach significance. The qualitative and quantitative distribution of individual gangliosides in Wt and R6/1 Tg mice is shown in Fig. 3b and Table 1. The content of all major gangliosides, with the exception of GD3, was significantly less in the R6/1 Tg mice than in the Wt mice ($p < 0.05$). The reductions in GM1, GD1a, GD1b, GT1b, and GQ1b were similar in the R6/1 Tg mice, ranging from 22 to 36%. LD1, however, showed the greatest reduction and was 62% less in the R6/1 Tg mice than in the Wt mice. LD1 (NeuAc-NeuAcα2-3Galβ1-4GlcNAcβ1-3Galβ1-4Glc1-1Cer) is a ganglioside that is highly enriched in Purkinje cells and migrates with GT1a in a chloroform/methanol/0.25% aqueous $CaCl_2$ developing solvent system (Chou *et al.* 1990).

The qualitative and quantitative distribution of cerebellar neutral and acidic lipids in the Wt and the R6/1 Tg mice is shown in Fig. 4a and b, and Table 2. The myelin-enriched lipids, cerebrosides and sulfatides, were reduced in the R6/1 Tg mice when compared with the Wt mice. This difference was significant for sulfatides (13% reduction) ($p < 0.05$) and no overlap was observed in the two independent samples for cerebrosides, representing a 26% reduction. These findings indicate that the R6/1 Tg mice have significant reductions in cerebellar total ganglioside content, in ganglioside distribution, and in myelin-enriched sulfatides when compared with the Wt mice. Furthermore, these data suggest an association between loss of motor function, Purkinje cell abnormality, reduced GSL gene expression, and cerebellar lipid abnormalities.

GSL gene expression in control and Huntington's disease subjects

To determine whether the changes observed in the R6/1 Tg mice represent an undiscovered feature of pathology in human HD, we next performed qPCR for selected genes on isolated human cerebellar RNA. In accord with the R6/1 Tg mice, Galgt1 was significantly reduced in the cerebellum of HD subjects when compared with control subjects ($p = 0.03$) (Fig. 5a). Moreover, SiaT8a (GD3 synthase) and SiaT9 (GM3 synthase) were also significantly reduced in the cerebellum of HD subjects when compared with control subjects ($p < 0.04$).

Cerebellar lipids of control and Huntington's disease subjects

We next analyzed the qualitative (Fig. 5b) and quantitative (Table 1) distribution of individual gangliosides in human post-mortem cerebellum samples from HD and control subjects. We processed three HD cerebellum samples, pathology grade 3, which were age and sex matched to three controls samples. The content and distribution of cerebellar gangliosides in the control subjects was generally similar to that reported previously for normal human cerebellum (Brooksbank and McGovern 1989). In addition, cerebellar ganglioside content and distribution was generally similar in

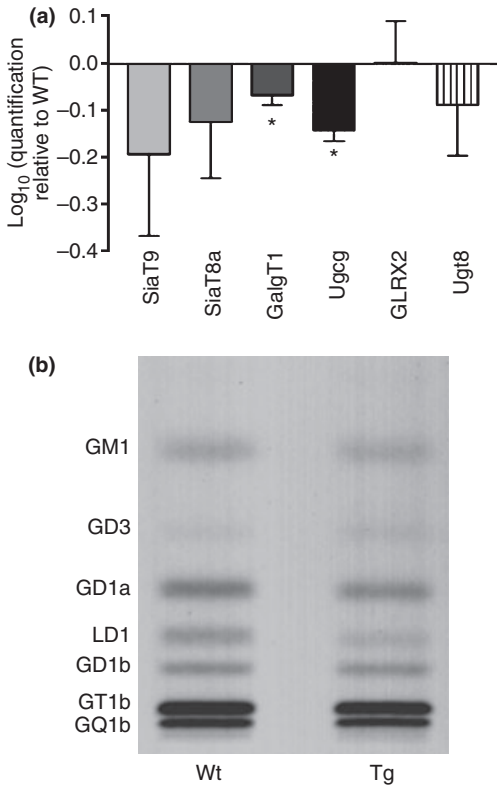

Fig. 3 Gene expression levels of ganglioside-metabolism enzymes in cerebellum of R6/1 Tg mice (a). qPCR amplification of the indicated transcripts from the cerebellum of symptomatic R6/1 Tg mice and Wt littermate controls. Values are expressed as the averages of the $2\exp(C_t)$ ± SEM of duplicate determinations from two independent experiments ($n = 5$ mice/group). Amplification of the hypoxanthine guanine phosphoribosyl transferase (Hprt) housekeeping gene was used as an internal reference and the expression level from the Wt mice was used as calibrator in the ΔCt method. *$p < 0.05$. HPTLC of cerebellar gangliosides in R6/1 mice (b). The amount of ganglioside sialic acid spotted per lane was equivalent to approximately 1.5 μg. The plate was developed by a single ascending run with $CHCl_3$: CH_3OH : dH_2O (55 : 45 : 10 by vol) containing 0.02% $CaCl_2{\cdot}2H_2O$. The bands were visualized with resorcinol – HCl spray.

our control subjects and in the Wt mice analyzed (Table 1). Total cerebellar ganglioside concentration was not significantly different between HD and control subjects. The levels of all major gangliosides, with the exception of GQ1b and GD3, were, on average, higher in the HD subjects than in the control subjects. GM1 was significantly greater in the cerebellum of HD subjects than in control subjects ($p < 0.05$).

The qualitative and quantitative distribution of cerebellar neutral and acidic lipids in the control and the HD subjects is shown in Fig. 6a and b, and Table 2. Similar to human postmortem caudate samples (Desplats *et al.* 2007), no significant differences were observed between the control and the HD subjects for the distribution of these cerebellar lipids, to include cholesterol and white matter-enriched glycolipids, cerebrosides and sulfatides. These findings indicate that the HD and control subjects have similar levels of total cerebellar ganglioside content and of the content of individual gangliosides, with the exception of GM1, without noticeable alterations in neutral or acidic lipids.

Discussion

In this study, we detected abnormal gait patterns in R6/1 Tg mice that were reminiscent of those seen in human Huntington's disease (HD) patients. R6/1 Tg mice displayed a markedly decreased performance when compared with Wt mice in a footprint analysis that was similar to the performance of its sister transgenic line, the R6/2 Tg mice (Carter *et al.* 1999). Moreover, we demonstrated significant decreases in the levels of mRNAs encoding enzymes involved glycosphingolipid (GSL) metabolism in the cerebellum of R6/1 Tg mice, and a decrease in the number and structure of Purkinje cells in the cerebellum of R6/1 Tg mice. Although we show a severely abnormal cerebellar distribution of gangliosides in R6/1 Tg mice, similar abnormalities were not found in cerebellar samples from the human HD subjects.

Although the caudate and putamen have been the main focus of much HD research, lesions have also been reported, albeit to a much lesser extent, in the cerebellum and brainstem (Rodda 1981; Hattori *et al.* 1984). Cerebellar abnormalities have often been associated with juvenile cases (Hattori *et al.* 1984; Ruocco *et al.* 2006; Sakazume *et al.* 2009) and in adults, can often precede the changes seen in the striatum. HD belongs to a group of triple repeat (CAG) disorders that includes dentatorubropallidoluysian atrophy (DRPLA), spinocerebellar ataxia, and spinobulbar muscular atrophy. All of these diseases exhibit cerebellar manifestations. Cerebellar gray and white matter volumes have been reported to be smaller in HD subjects than in control subjects (Ruocco *et al.* 2006; Paradiso *et al.* 2008), and an imaging study has recently shown significant decreases in both gray and white matter in the cerebellum (Fennema-Notestine *et al.* 2004). Furthermore, Jech *et al.* (2007) reported that the CAG number correlated inversely with white matter intensity in the right HD cerebellum. Although there seems to be a plentitude of data suggesting that HD is a multisystem disorder with involvement from the cerebellum, there has been no mechanistic approach to investigating cerebellar biochemistry in HD.

In the present study, we observed significant reductions in the levels in the expression of two genes encoding two glycosyltransferases Ugcg and Galgt1 in the cerebellum of R6/1 Tg mice. First, we found a significant decrease in Ugcg, the gene encoding glucosylceramide synthase (UDP-glucose : ceramide glucosyltransferase). Glucosylceramide synthase modifies ceramide with the transfer of glucose from UDP-glucose to produce glucosylceramide. Following

Table 1 Total ganglioside content and distribution in cerebellum of R6/1 mice and HD subjects[a]

	Mice[b]			Human		
Genotype	Wt	Tg	Difference (%)	Control	HD	Difference (%)
Age	7–8 months	7–8 months	–	49,58,55 years	46,53,54 years	
Sex	F	F		M,F,M	M,F,M	
Wet weight (mg)	64.1 ± 2.0	53.2 ± 0.6*	−17	–	–	
Water content (%)	77.9 ± 0.5	78.9 ± 0.2	1	–	–	
Ganglioside content (μg sialic acid/100 mg dry weight)[c]						
Total	346 ± 4	242 ± 12*	−30	357 ± 33	443 ± 99	24
GM1	27.4 ± 1.6	17.6 ± 1.6*	−36	17.7 ± 2.4	30.6 ± 3.8*	73
GD3	7.1 ± 0.9	6.3 ± 0.3	−11	30.5 ± 13.2	27.7 ± 7.8	−9
GD1a	43.1 ± 2.2	28.9 ± 0.9**	−33	36.6 ± 3.5	60.7 ± 20.7	66
LD1[d]	22.0 ± 1.7	8.4 ± 0.7**	−62	–	–	–
GD2	–	–	–	11.3 ± 1.9	28.8 ± 10.0	155
GD1b	21.3 ± 0.8	16.7 ± 0.7*	−22	63.3 ± 3.6	90.2 ± 26.9	42
GT1b	138 ± 2.6	98.1 ± 4.8**	−29	145.9 ± 14.4	159.8 ± 49.4	10
GQ1b	86.9 ± 2.1	66.3 ± 3.2**	−24	51.4 ± 11.5	45.1 ± 3.1	−12

[a]Values represent the mean ± SEM of three independent mice/group or three independent human subjects/group.
[b]Wt and Tg represent wild-type and R6/1 transgenic mice, respectively.
[c]Determined from densitometric scanning of HPTLC as shown in Figs 3 and 5.
[d]LD1 represents disialosylparagloboside.
The value is significantly different from that of the control group at *$p < 0.05$ and **$p < 0.01$ as determined from the two-tailed *t*-test.

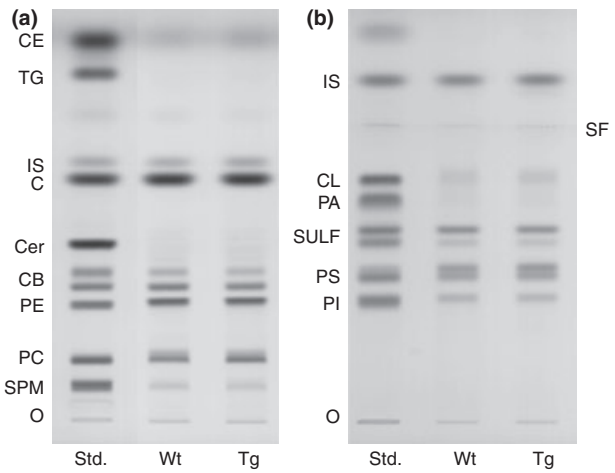

Fig. 4 High-performance TLC of cerebellar neutral (a) and acidic lipids (b) in R6/1 mice. The amount of neutral and acidic lipids spotted per lane was equivalent to approximately 70 and 200 mg tissue dry weight, respectively. The plates were developed as described in Materials and methods section. CE, cholesteryl esters; TG, triglycerides; IS, internal standard; C, cholesterol; Cer, ceramide; CB, cerebrosides (doublet); PE, phosphatidylethanolamine; PC, phosphatidylcholine; SPM, sphingomyelin; FA, fatty acids; IS, internal standard; CL, cardiolipin; PA, phosphatidic acid; SULF, sulfatides (doublet); PS, phosphatidylserine; PI, phosphatidylinositol; O, origin; SF, solvent front of the first developing solvent system.

the addition of a galactose moiety and a sialic acid, GM3, the first ganglioside in the ganglioside synthesis pathway, is produced. Secondly, we found a significant decrease in Galgt1 (*GalNAcT*), the gene which encodes for β-1,4-*N*-acetylgalactosaminyltransferase, the enzyme that is required for the synthesis of complex gangliosides. Mice that are homozygous for a disrupted *GalNAcT* gene are deficient in complex gangliosides and express predominantly the simple gangliosides GM3 and GD3 (Takamiya *et al.* 1996; Liu *et al.* 1997). Moreover, the simple gangliosides GM3 and GD3 are expressed at much higher levels in $GalNAcT^{-/-}$ mice than in Wt mice (Takamiya *et al.* 1996). We, therefore, predicted that with significantly less Ugcg, all gangliosides in the cerebellum of R6/1 Tg mice would be reduced because they are downstream of GM3 in the ganglioside synthetic pathway (Kasperzyk *et al.* 2004). Although our data are mostly in accord with our prediction, we did not see a significant decrease in cerebellar GD3 in R6/1 Tg mice. We hypothesized, that similar to the $GalNAcT^{-/-}$ mice, there might be some compensatory increase in simple gangliosides (e.g. GD3) when complex gangliosides are dramatically decreased. Furthermore, as there is some glycosyltransferase activity in the R6/1 Tg mice, this residual activity might allow for the production of the complex gangliosides. It is interesting to note that unlike the $GalNAcT^{-/-}$, the R6/1 Tg mice have significantly less complex gangliosides without having a dramatic increase in simple gangliosides and therefore, may be a useful model in investigating gangliosides in neural development.

The myelin-enriched ganglioside GM1 was the second most significantly decreased ganglioside in the cerebellum of R6/1 Tg mice when compared with Wt mice. This decrease

Table 2 Neutral and acidic lipid distribution in cerebellum of R6/1 mice and HD subjects[a]

Genotype	Mice		Human	
	Wt	Tg	Control	HD
	(mg/100 mg dry weight)[b]			
Neutral lipids				
Cholesterol	4.0 (4.0, 4.0)	3.7 (3.7, 3.7)	5.4 ± 0.4	6.6 ± 1.3
Cerebrosides	1.9 (1.8, 1.9)	1.4 (1.4, 1.5)	2.8 ± 0.6	4.8 ± 2.3
Phosphatidylethanolamine	3.2 (3.2, 3.2)	2.8 (2.8, 2.8)	7.5 ± 0.5	8.4 ± 0.8
Phosphatidylcholine	2.5 (2.4, 2.5)	2.5 (2.5, 2.5)	4.3 ± 0.5	4.1 ± 0.3
Sphingomyelin	0.3 (0.3, 0.3)	0.2 (0.2, 0.2)	1.7 ± 0.1	2.6 ± 0.8
Acidic lipids				
Cardolipin	0.50 ± 0.02	0.64 ± 0.10	0.4 ± 0.1	0.8 ± 0.4
Sulfatides	1.12 ± 0.01	0.96 ± 0.04*	1.0 ± 0.3	1.4 ± 0.6
Phosphatidylserine	2.05 ± 0.09	2.01 ± 0.10	2.1 ± 0.2	2.0 ± 0.3
Phosphatidylinositol	0.71 ± 0.04	0.64 ± 0.04	0.6 ± 0.0	0.6 ± 0.0

[a]Values represent the mean ± SEM of three independent mice/group or three independent human subjects/group, unless indicated otherwise.
[b]Determined from densitometric scanning of HPTLC as shown in Figs 4 and 6.
*The value is significantly different from that of the Wt mice at $p < 0.05$ as determined from the two-tailed *t*-test.

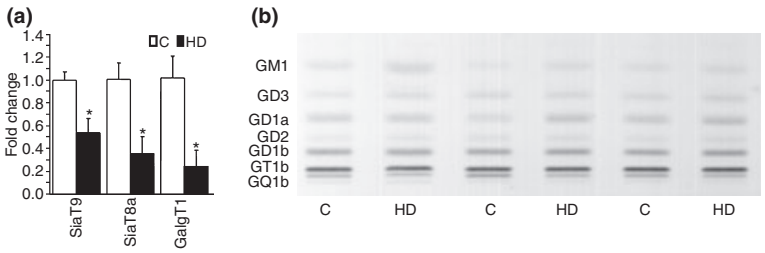

Fig. 5 Gene expression levels of ganglioside-metabolism enzymes in the cerebellum of post-mortem HD subjects (a). qPCR amplification of the indicated transcripts from cerebellum of control and HD subjects. Values are expressed as the averages of the $2\exp(C_t)$ ± SEM of duplicate determinations from two independent experiments ($n = 3$ subjects/group). HD cerebella were a pathological grade 3. Amplification of β-2-microglobulin (B2M) housekeeping gene was used as an internal reference and the expression level from the control subjects was used as calibrator in the ΔC_t method. *$p < 0.05$. High-performance TLC of cerebellar gangliosides in HD subjects (b). The amount of ganglioside sialic acid spotted per lane was equivalent to approximately 1.5 μg. The plate was developed by a single ascending run with $CHCl_3$: CH_3OH : dH_2O (55 : 45 : 10 by vol) containing 0.02% $CaCl_2{\cdot}2H_2O$. The bands were visualized with resorcinol–HCl spray.

may result from lower myelin levels or from demyelination, as sulfatides were also significantly reduced, and/or as a result of decreased levels of its synthesis enzyme. We previously found GM1 to be significantly reduced in the forebrain (cortex and striatum pooled) of R6/1 Tg mice when compared with Wt mice (Desplats *et al.* 2007). Moreover, a recent study using an alternative HD murine model, the YAC128 mice, also found a significant decrease in GM1 in striatum and cortex, and additionally, significant decreases in GT1b and GD1a in striatum and cortex, respectively (Maglione *et al.* 2010). The synthesis of GM1 was also reduced in fibroblasts from HD patients, most notably in a patient who did not manifest HD until 15 years after the biopsy was taken. The authors attribute the decrease in gangliosides as a reflection of the activity of metabolic pathways, rather than to the loss of neurons or accumulation of reactive glia. Our findings in the R6/1 Tg mice would support this contention because we did not find an elevation of ganglioside GD3, a ganglioside which becomes elevated in reactive glia in association with post-maturation neurodegeneration in mouse cerebellum (Seyfried *et al.* 1984b; Seyfried and Yu 1985). In light of these facts, our findings suggest that the marked reductions in total cerebellar ganglioside content could result more from failures in ganglioside biosynthesis than from neurodegeneration. The reduction in myelin-enriched cerebrosides and sulfatides could also be secondary consequences of abnormal GSL biosynthesis. Further studies will be needed to test this hypothesis.

Although we maintain that the severe ganglioside abnormalities are caused by reductions in glycosyltransferases, we do not exclude the possibility that the severe ganglioside

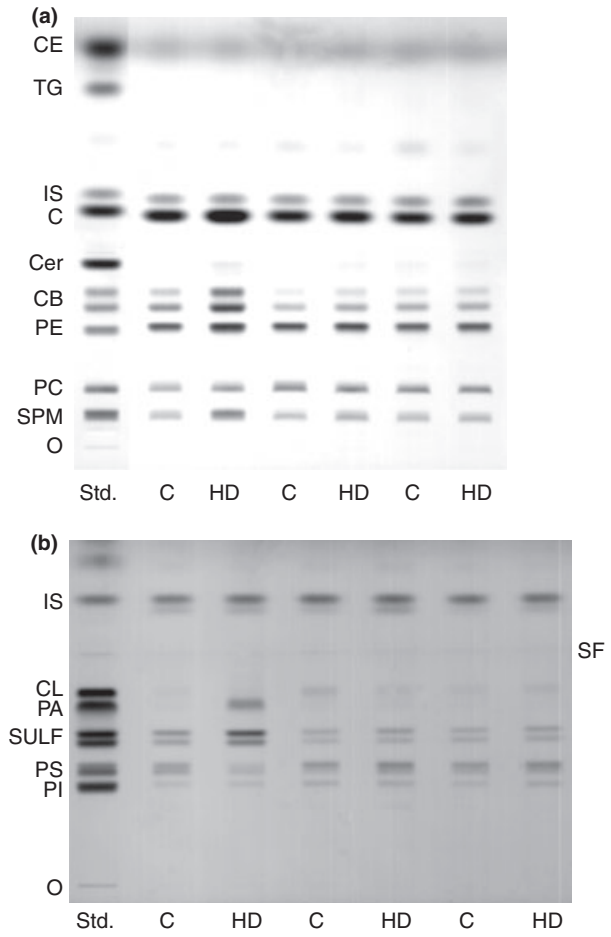

Fig. 6 High-performance TLC of neutral lipids (a), and acidic lipids (b) in HD subjects. The amount of neutral and acidic lipids spotted per lane was equivalent to approximately 40 and 75 μg tissue dry weight, respectively. The plates were developed as described in Materials and methods section. CE, cholesteryl esters; TG, triglycerides; IS, internal standard; C, cholesterol; Cer, ceramide; CB, cerebrosides (doublet); PE, phosphatidylethanolamine; PC, phosphatidylcholine; SPM, sphingomyelin; CL, cardiolipin; PA, phosphatidic acid; SULF, sulfatides (doublet); PS, phosphatidylserine; PI, phosphatidylinositol; O, origin; SF, solvent front of the first developing solvent system.

reductions seen in the R6/1 Tg mice could also be partially attributed to the loss of neurons in which they are enriched. However, R6/1 and related lines do not show neuronal loss, despite overall atrophy (Mangiarini *et al.* 1996). As GD3 was not elevated, it is unlikely that neuron loss occurred after neuronal differentiation, as we have previously described (Seyfried *et al.* 1984b). Conversely, in accord with a previous cerebellar HD human study (Jeste *et al.* 1984), we report here a decrease in the number of Purkinje cells, and LD1 as the most significantly reduced ganglioside. LD1 (NeuAc-NeuAcα2-3Galβ1-4GlcNAcβ1-3Galβ1-4Glc1-1Cer) is a ganglioside highly enriched in Purkinje cells and migrates with GT1a in a chloroform/methanol/0.25% aqueous $CaCl_2$ developing solvent system (Chou *et al.* 1990). In conclusion, we contend that the massive reductions in cerebellar gangliosides in R6/1 Tg mice are most likely caused by: (i) mainly reduced glycosyltransferase expression, and (ii) to a lesser extent, cell death or activation of inflammatory processes.

The cerebellum lipid abnormalities in the R6/1 Tg mice were not seen in the human HD subjects even though the content and composition of cerebellar lipids were generally similar in Wt mice and in control human subjects. Cerebellar gangliosides were similar in the HD subjects when compared with the control subjects, with the exception of GM1, which was significantly elevated in HD subjects ($p < 0.05$). The acidic and neutral cerebellar lipids profiles were also similar in control and HD subjects, suggesting that in these particular HD cerebellar samples, there is, in fact, an increase in cerebellar gangliosides. Conversely, the reductions in glycosyltransferase expression seen in the R6/1 Tg mice (e.g. Galgt1) were seen in the HD subjects (e.g. Galgt1, SiaT8a, SiaT9). This is surprising since one would expect major ganglioside reductions to follow decreases in these glycosyltransferases. We theorize that unlike the R6/1 Tg mice, which most likely have GSL abnormalities throughout life, the HD subjects may only have decreased levels of glycosyltransferases when symptomatology begins later on in life. The turnover rate of gangliosides might be slower in aged patients, and therefore, might not reflect a change in the glycosyltransferase expression pattern.

If cerebellar gangliosides are indeed increased in some HD subjects, we must then ask why this particular area would have increased gangliosides when all other cerebral brain regions analyzed have decreased gangliosides (Bernheimer *et al.* 1979; Desplats *et al.* 2007)? One explanation is that some functional derangement has occurred in the cerebellum because of the profound movement abnormalities observed in HD. As the cerebellum's main function is to govern and coordinate the movements of the muscular system, the irregular, ungoverned movements in chorea or gait disturbances could originate in the cerebellum. The elevated level of total cerebellar ganglioside content in the HD subjects would be expected since with chorea, neurons receive excessive activation and stimulation, as has been seen with epilepsy (Brigande *et al.* 1992). We suggest that these irregular, jerky movements would most likely require synaptogenesis, neurite outgrowth, and cellular growth, not necessarily in an organized, jointed manner, and therefore, require increased ganglioside biosynthesis. Further studies will be necessary to determine how the motor abnormalities expressed in HD subjects might alter ganglioside biosynthesis.

Comparison between the R6/1 Tg mice and HD subjects is not ideal in this particular study, as the human sample size is small. However, we would like to point out reasons why we attribute the lack of correlation in the lipid profiles, which is

summarized in the following possibilities: (i) The current mouse models of HD, including the R6/1 Tg mice, do not mimic all aspects of the severe neurodegenerative changes observed in human HD. Interestingly, only some of the HD mouse models show slight neuronal loss in the striatum, the most commonly seen symptom of HD (Mangiarini *et al.* 1996; Hodgson *et al.* 1999). Although our current and previous findings (Desplats *et al.* 2007) highlight the significance of GSL abnormalities in the human disease, they highlight the dearth of an accurate and appropriate HD mouse model to assess cerebellar function. (ii) Our current and past studies (Desplats *et al.* 2007) have included a small human sample. Although these studies have proved to be extremely informative, we suggest that further quantitative analyses with a larger number of human samples with varying grades (0–3 pathology) is needed to fully assess the impact of disrupted GSL metabolism on HD cerebellar pathology. Moreover, juvenile HD cerebellar samples would be of interest, as those cases would more likely include cerebellar GSL anomalies. (iii) Lastly, considerable variability in cerebellar pathology is known to occur in HD patients. Although we included grade 3 pathology samples in our analysis, we are limited in knowing the extent of cerebellar involvement in these specific cases.

In conclusion, we report altered motor behavior and abnormal expression of genes encoding glycosyltransferases in the R6/1 Tg mouse model of HD. The content of most major cerebellar gangliosides was significantly less in R6/1 Tg mice when compared with Wt mice. In contrast to the ganglioside reductions observed in the R6/1 Tg mice, total cerebellar ganglioside content and distribution of individual gangliosides was similar in HD and control subjects, with the exception of GM1, which was significantly elevated in HD subjects. Although the cerebellar lipid changes found in the R6/1 Tg mice did not mimic those found in our HD subjects, further studies will be necessary to assess cerebellar GSLs in HD. We suggest that the R6/1 Tg mice may prove to be extremely useful for evaluating the role of GSLs not only in cerebellar development, but also in the morphogenesis and organogenesis of the brain.

Acknowledgements

We thank Youngho P. Kim for technical assistance and Karie Heinecke for assistance in manuscript preparation. The work was supported in part by NIH grants HD39722, NS44169, and MH069696, the Boston College Research Expense Fund, and the National Tay-Sachs and Allied Disease Association Inc. (NTSAD). The authors declare that they have no financial conflicts of interest.

References

Ando S., Chang N. C. and Yu R. K. (1978) High-performance thin-layer chromatography and densitometric determination of brain gangliosides compositions of several species. *Anal. Biochem.* **89**, 437–450.

Bates G. P. (2001) Huntington's disease. Exploiting expression. *Nature* **413**(691), 693–694.

Bernheimer H., Sperk G., Price K. S. and Hornykiewicz O. (1979) Brain gangliosides in Huntington's Disease. *Adv. Neurol.* **23**, 463–471.

Bolivar V. J., Manley K. and Messer A. (2004) Early exploratory behavior abnormalities in R6/1 Huntington's disease transgenic mice. *Brain Res.* **1005**, 29–35.

Brigande J. V., Wieraszko A., Albert M. D., Balkema G. W. and Seyfried T. N. (1992) Biochemical correlates of epilepsy in the E1 mouse: analysis of glial fibrillary acidic protein and gangliosides. *J. Neurochem.* **58**, 752–760.

Brooksbank B. W. and McGovern J. (1989) Gangliosides in the brain in adult Down's syndrome and Alzheimer's disease. *Mol. Chem. Neuropathol.* **11**, 143–156.

Byers R. K., Gilles F. H. and Fung C. (1973) Huntington's disease in children. Neuropathologic study of four cases. *Neurology* **23**, 561–569.

Byrne M. C., Farooq M., Sbaschnig-Agler M., Norton W. T. and Ledeen R. W. (1988) Ganglioside content of astroglia and neurons isolated from maturing rat brain: consideration of the source of astroglial gangliosides. *Brain Res.* **461**, 87–97.

Carter R. J., Lione L. A., Humby T., Mangiarini L., Mahal A., Bates G. P., Dunnett S. B. and Morton A. J. (1999) Characterization of progressive motor deficits in mice transgenic for the human Huntington's disease mutation. *J. Neurosci.* **19**, 3248–3257.

Chou D. K., Flores S. and Jungalwala F. B. (1990) Identification of disialosyl paragloboside and *O*-acetyldisialosyl paragloboside in cerebellum and embryonic cerebrum. *J. Neurochem.* **54**, 1598–1607.

Denny C. A., Kasperzyk J. L., Gorham K. N., Bronson R. T. and Seyfried T. N. (2006) Influence of caloric restriction on motor behavior, longevity, and brain lipid composition in Sandhoff disease mice. *J. Neurosci. Res.* **83**, 1028–1038.

Desplats P. A., Kass K. E., Gilmartin T., Stanwood G. D., Woodward E. L., Head S. R., Sutcliffe J. G. and Thomas E. A. (2006) Selective deficits in the expression of striatal-enriched mRNAs in Huntington's disease. *J. Neurochem.* **96**, 743–757.

Desplats P. A., Denny C. A., Kass K. E., Gilmartin T., Head S. R., Sutcliffe J. G., Seyfried T. N. and Thomas E. A. (2007) Glycolipid and ganglioside metabolism imbalances in Huntington's disease. *Neurobiol. Dis.* **27**, 265–277.

DiFiglia M., Sapp E., Chase K. O., Davies S. W., Bates G. P., Vonsattel J. P. and Aronin N. (1997) Aggregation of huntingtin in neuronal intranuclear inclusions and dystrophic neurites in brain. *Science* **277**, 1990–1993.

Fennema-Notestine C., Archibald S. L., Jacobson M. W., Corey-Bloom J., Paulsen J. S., Peavy G. M., Gamst A. C., Hamilton J. M., Salmon D. P. and Jernimangan T. L. (2004) In vivo evidence of cerebellar atrophy and cerebral white matter loss in Huntington disease. *Neurology* **63**, 989–995.

Furuya S., Irie F., Hashikawa T., Nakazawa K., Kozakai A., Hasegawa A., Sudo K. and Hirabayashi Y. (1994) Ganglioside GD1 alpha in cerebellar Purkinje cells. Its specific absence in mouse mutants with Purkinje cell abnormality and altered immunoreactivity in response to conjunctive stimuli causing long-term desensitization. *J. Biol. Chem.* **269**, 32418–32425.

Gusella J. F., Wexler N. S. and Conneally P. M. *et al.* (1983) A polymorphic DNA marker genetically linked to Huntington's disease. *Nature* **306**, 234–238.

Harper P. S. (1996) New genes for old diseases: the molecular basis of myotonic dystrophy and Huntington's disease. The Lumleian Lecture 1995. *J. R. Coll. Physicians Lond.* **30**, 221–231.

Hattori H., Takao T., Ito M., Nakano S., Okuno T. and Mikawa H. (1984) Cerebellum and brain stem atrophy in a child with Huntington's chorea. *Comput. Radiol.* **8**, 53–56.

Hauser E. C., Kasperzyk J. L., d'Azzo A. and Seyfried T. N. (2004) Inheritance of lysosomal acid beta-galactosidase activity and gangliosides in crosses of DBA/2J and knockout mice. *Biochem. Genet.* **42**, 241–257.

Hayden M. R. and Kremer B. (1995) Huntington disease. in *The Metabolic and Molecular Bases of Inherited Disease* (Scriver C. R., Beaudet A. L., Sly W. S. and Valle D., eds), Vol. III, pp. 4483–4510. McGraw-Hill, New York.

Hodgson J. G., Agopyan N. and Gutekunst C. A. *et al.* (1999) A YAC mouse model for Huntington's disease with full-length mutant huntingtin, cytoplasmic toxicity, and selective striatal neurodegeneration. *Neuron* **23**, 181–192.

Imarisio S., Carmichael J. and Korolchuk V. *et al.* (2008) Huntington's disease: from pathology and genetics to potential therapies. *Biochem. J.* **412**, 191–209.

Jech R., Klempír J., Vymazal J., Zidovská J., Klempírová O., Ruzicka E. and Roth J. (2007) Variation of selective gray and white matter atrophy in Huntington's disease. *Mov. Disord.* **22**, 1783–1789.

Jervis G. A. (1963) Huntington's chorea in childhood. *Arch. Neurol.* **9**, 244–257.

Jeste D. V., Barban L. and Parisi J. (1984) Reduced Purkinje cell density in Huntington's disease. *Exp. Neurol.* **85**, 78–86.

Kasperzyk J. L., El-Abbadi M. M., Hauser E. C., D'Azzo A., Platt F. M. and Seyfried T. N. (2004) N-butyldeoxygalactonojirimycin reduces neonatal brain ganglioside content in a mouse model of GM1 gangliosidosis. *J. Neurochem.* **89**, 645–653.

Kasperzyk J. L., d'Azzo A., Platt F. M., Alroy J. and Seyfried T. N. (2005) Substrate reduction reduces gangliosides in postnatal cerebrum-brainstem and cerebellum in GM1 gangliosidosis mice. *J. Lipid Res.* **46**, 744–751.

Ledeen R. W. (1983) Gangliosides, in *Handbook of Neurochemistry* (Lajtha e. A., ed.), Vol. 3, pp. 41–90. Plenum Publishing Co., New York.

LeVine S. M. and Goldman J. E. (1988) Spatial and temporal patterns of oligodendrocyte differentiation in rat cerebrum and cerebellum. *J. Comp. Neurol.* **277**, 441–455.

Liu Y., Hoffmann A., Grinberg A., Westphal H., McDonald M. P., Miller K. M., Crawley J. N., Sandhoff K., Suzuki K. and Proia R. L. (1997) Mouse model of GM2 activator deficiency manifests cerebellar pathology and motor impairment. *Proc. Natl Acad. Sci. USA* **94**, 8138–8143.

Macala L. J., Yu R. K. and Ando S. (1983) Analysis of brain lipids by high performance thin-layer chromatography and densitometry. *J. Lipid Res.* **24**, 1243–1250.

MacDonald M. E. (2003) Huntingtin: alive and well and working in middle management. *Sci. STKE* **2003**, pe48.

MacDonald M. E., Gines S., Gusella J. F. and Wheeler V. C. (2003) Huntington's disease. *Neuromol. Med.* **4**, 7–20.

Maglione V., Marchi P., Di Pardo A., Lingrell S., Horkey M., Tidmarsh E. and Sipione S. (2010) Impaired ganglioside metabolism in Huntington's disease and neuroprotective role of GM1. *J. Neurosci.* **30**, 4072–4080.

Mangiarini L., Sathasivam K. and Seller M. *et al.* (1996) Exon 1 of the HD gene with an expanded CAG repeat is sufficient to cause a progressive neurological phenotype in transgenic mice. *Cell* **87**, 493–506.

Markham C. H. (1969) Huntington's chorea in childhood, in *Neurogenetics* (Barbeau A and Brunette IR, eds), Vol. 1, pp. 645–650. Excerpta Medica, Amsterdam.

Muse E. D., Jurevics H., Toews A. D., Matsushima G. K. and Morell P. (2001) Parameters related to lipid metabolism as markers of myelination in mouse brain. *J. Neurochem.* **76**, 77–86.

Naver B., Stub C., Moller M., Fenger K., Hansen A. K., Hasholt L. and Sorensen S. A. (2003) Molecular and behavioral analysis of the R6/1 Huntington's disease transgenic mouse. *Neuroscience* **122**, 1049–1057.

Paradiso S., Turner B. M., Paulsen J. S., Jorge R., Boles Ponto L. L. and Robinson R. G. (2008) Neural bases of dysphoria in early Huntington's disease. *Psychiatry Res.* **162**, 73–87.

Raff M. C., Abney E. R., Cohen J., Lindsay R. and Noble M. (1983) Two types of astrocytes in cultures of developing rat white matter: differences in morphology, surface gangliosides, and growth characteristics. *J. Neurosci.* **3**, 1289–1300.

Rodda R. A. (1981) Cerebellar atrophy in Huntington's disease. *J. Neurol. Sci.* **50**, 147–157.

Ruocco H. H., Lopes-Cendes I., Laurito T. L., Li L. M. and Cendes F. (2006) Clinical presentation of juvenile Huntington disease. *Arq. Neuropsiquiatr.* **64**, 5–9.

Sakazume S., Yoshinari S., Oguma E., Utsuno E., Ishii T., Narumi Y., Shiihara T. and Ohashi H. (2009) A patient with early onset Huntington disease and severe cerebellar atrophy. *Am. J. Med. Genet. Part A* **149A**, 598–601.

Seyfried T. N. (1979) Audiogenic seizures in mice. *Fed. Proc.* **38**, 2399–2404.

Seyfried T. N. and Yu R. K. (1980) Heterosis for brain myelin content in mice. *Biochem. Genet.* **18**, 1229–1237.

Seyfried T. N. and Yu R. K. (1984) Cellular localization of gangliosides in the mouse cerebellum: analysis using neurological mutants. *Adv. Exp. Med. Biol.* **174**, 169–181.

Seyfried T. N. and Yu R. K. (1985) Ganglioside GD3: structure, cellular distribution, and possible function.. *Mol. Cell. Biochem.* **68**, 3–10.

Seyfried T. N. and Yu R. K. (1990) Cerebellar ganglioside abnormalities in pcd mutant mice. *J. Neurosci. Res.* **26**, 105–111.

Seyfried T. N., Glasher G. H. and Yu R. K. (1978) Cerebral, cerebellar, and brain stem gangliosides in mice susceptible to audiogenic seizures. *J. Neurochem.* **31**, 21–27.

Seyfried T. N., Miyazawa N. and Yu R. K. (1983) Cellular localization of gangliosides in the developing mouse cerebellum: analysis using the weaver mutant. *J. Neurochem.* **41**, 491–505.

Seyfried T. N., Bernard D., Mayeda F., Macala L. and Yu R. K. (1984a) Genetic analysis of cerebellar lipids in mice susceptible to audiogenic seizures. *Exp. Neurol.* **84**, 590–595.

Seyfried T. N., Bernard D. J. and Yu R. K. (1984b) Cellular distribution of gangliosides in the developing mouse cerebellum: analysis using the staggerer mutant. *J. Neurochem.* **43**, 1152–1162.

Takamiya K., Yamamoto A. and Furukawa K. *et al.* (1996) Mice with disrupted GM2/GD2 synthase gene lack complex gangliosides but exhibit only subtle defects in their nervous system. *Proc. Natl Acad. Sci. USA* **93**, 10662–10667.

The Huntington's Disease Collaborative Research Group. (1993) A novel gene containing a trinucleotide repeat that is expanded and unstable on Huntington's disease chromosomes. The Huntington's Disease Collaborative Research Group. *Cell* **72**, 971–983.

Trottier Y., Devys D., Imbert G., Saudou F., An I., Lutz Y., Weber C., Agid Y., Hirsch E. C. and Mandel J. (1995) Cellular localization of the Huntington's disease protein and discrimination of the normal and mutated form. *Nat. Genet.* **10**, 104–110.

Vonsattel J. P. and DiFiglia M. (1998) Huntington disease. *J. Neuropathol. Exp. Neurol.* **57**, 369–384.